

# 1 **pyControl: Open source, Python based, hardware and software for** 2 **controlling behavioural neuroscience experiments.**

3 Thomas Akam<sup>1,2\*</sup>, Andy Lustig<sup>3</sup>, James Rowland<sup>4</sup>, Sampath K.T. Kapaniah<sup>5</sup>, Joan Esteve-Agraz<sup>6</sup>,  
4 Mariangela Panniello<sup>4,7</sup>, Cristina Marquez<sup>6</sup>, Michael Kohl<sup>4,7</sup>, Dennis Kätzel<sup>5</sup>, Rui M. Costa<sup>†,2,8</sup>, Mark  
5 Walton<sup>†,1</sup>

6 1. Department of Experimental Psychology, University of Oxford, Oxford, UK

7 2. Champalimaud Neuroscience Program, Champalimaud Centre for the Unknown, Lisbon, Portugal

8 3. Janelia Research Campus, Howard Hughes Medical Institute, Ashburn, VA, USA

9 4. Department of Physiology Anatomy & Genetics, University of Oxford, Oxford, UK

10 5. Institute of Applied Physiology, Ulm University, Germany

11 6. Instituto de Neurociencias (Universidad Miguel Hernández-Consejo Superior de Investigaciones  
12 Científicas), Sant Joan d'Alacant, Spain

13 7. Institute of Neuroscience and Psychology, University of Glasgow, Glasgow, UK

14 8. Department of Neuroscience and Neurology, Zuckerman Mind Brain Behavior Institute, Columbia  
15 University, New York, NY, USA.

16 † Equal contribution.

17 \* thomas.akam@psy.ox.ac.uk

## 18 **Abstract:**

19 Laboratory behavioural tasks are an essential research tool. As questions asked of behaviour  
20 and brain activity become more sophisticated, the ability to specify and run richly structured  
21 tasks becomes more important. An increasing focus on reproducibility also necessitates  
22 accurate communication of task logic to other researchers. To these ends we developed  
23 pyControl, a system of open source hardware and software for controlling behavioural  
24 experiments comprising; a simple yet flexible Python-based syntax for specifying tasks as  
25 extended state machines, hardware modules for building behavioural setups, and a graphical  
26 user interface designed for efficiently running high throughput experiments on many setups in  
27 parallel, all with extensive online documentation. These tools make it quicker, easier and  
28 cheaper to implement rich behavioural tasks at scale. As important, pyControl facilitates  
29 communication and reproducibility of behavioural experiments through a highly readable task  
30 definition syntax and self-documenting features.

## 31 **Resources:**

32 Documentation: <https://pycontrol.readthedocs.io>

33 Repositories: <https://github.com/pyControl>

34 User support: <https://groups.google.com/g/pycontrol>

35 **Introduction:**

36 Animal behaviour is of fundamental scientific interest, both in its own right and in relation to  
37 brain function (Krakauer et al., 2017). Though understanding natural behaviour is the ultimate  
38 goal, the tight control offered by laboratory tasks remains an essential tool in characterising  
39 learning mechanisms. To serve the needs of contemporary neuroscience, hardware and  
40 software for controlling behavioural experiments should be both flexible and easy to use.  
41 Additionally, an increasing focus on reproducibility (Baker, 2016; International Brain  
42 Laboratory et al., 2020) necessitates that behaviour control systems facilitate communication  
43 and replication of behavioural paradigms across labs.

44 Available commercial solutions often fall short of these desiderata. Proprietary closed-source  
45 hardware and software make it difficult to extend or adapt functionality beyond explicitly  
46 implemented use cases. Additionally, programming behavioural tasks on commercial systems  
47 can be surprisingly non-user-friendly, perhaps due to limitations of underlying legacy  
48 hardware. Commercial hardware is also typically very expensive considering the level of  
49 technology it represents, disadvantaging researchers outside well-funded institutions (Marder,  
50 2013; Chagas, 2018), and constraining the ability to scale behavioural assays for high  
51 throughput.

52 For these reasons, many groups implement their own behavioural hardware, either using low  
53 cost microcontrollers such as Arduinos or raspberry PI, or generic laboratory control software  
54 such as Labview (Devarakonda et al., 2016; O'Leary et al., 2018; Gurley, 2019; Bhagat et al.,  
55 2020; Buscher et al., 2020). Though highly flexible, building behavioural control systems from  
56 scratch has some disadvantages. It results in much duplication of effort as a lot of the required  
57 functionality is generic across experiments. Additionally, unless custom systems are well  
58 documented, it is hard for users to meaningfully share experimental protocols. This is  
59 important because scientific publications do not consistently contain sufficient information to  
60 constrain the details of the task used, yet such details are often crucial for reproducing the  
61 behaviour. Making task code public is therefore key to reproducibility, but this is only effective  
62 if it is readable and documented, as well as functional.

63 To address these limitations we developed *pyControl*; a system of open source hardware and  
64 software for controlling behavioural experiments. We report the design and rationale of  
65 system components, validation experiments characterising system performance, and  
66 behavioural data illustrating applications in 3 widely used, contrasting behavioural paradigms:  
67 5-choice serial reaction time task (5-CSRT) in operant chambers, sensory discrimination in  
68 head fixed animals, and a social decision-making task in a maze apparatus.

69

## 70 **Results:**

### 71 *System overview*

72 pyControl consists of three components, the pyControl framework, hardware, and graphical  
73 user interface (GUI). The framework implements the syntax used to program behavioural  
74 tasks. User-created task definition files, written in Python, run directly on microcontroller  
75 hardware, supported by framework code that determines when user-defined functions are  
76 called. This takes advantage of [Micropython](#), a recently developed port of the popular high-  
77 level language Python to microcontrollers. The framework handles functionality that is  
78 common across tasks, such as monitoring inputs, setting and checking timers, and streaming  
79 data back to the computer. This minimises boilerplate code in task files, while ensuring that  
80 common functionality is implemented reliably and efficiently. Combined with Python's highly  
81 readable syntax, this results in task files that are quick and straightforward to write, but also  
82 easy to read and understand (Figure 1), promoting replicability and communication of  
83 behavioural experiments.

84 pyControl hardware consists of a breakout board which interfaces a pyboard microcontroller  
85 with ports and connectors, and a set of devices such as nose-pokes, audio boards, LED  
86 drivers, rotary encoders, and stepper motor controllers that are connected to the breakout  
87 board to create behavioural setups. Breakout boards connect to the computer via USB, and  
88 many setups can be controlled in parallel from a single computer. pyControl implements a  
89 simple but robust mechanism for synchronising data with other systems such as cameras or  
90 physiology hardware. All hardware is fully open source, assembled hardware is available at  
91 low cost from the [Open Ephys store](#).

92 The GUI provides a graphical interface for setting up and running experiments, visualising  
93 behaviour and configuring setups, and is designed to facilitate high-throughput behavioural  
94 testing on many setups in parallel. To promote replicability, the GUI implements self-  
95 documenting features which ensure that all task files used to generate data are stored with  
96 the data itself, and that any changes to task parameters from default values are recorded in  
97 the data files.

### 98 *Task definition syntax*

99 Detailed information about task programming is provided in the [Programming Tasks](#)  
100 documentation. Here we give an overview of the task definition syntax and how this  
101 contributes to the flexibility of the system.

102 pyControl tasks are implemented as state machines, the basic elements of which are states  
103 and events. At any given time, the task is in one of the states, and the current state determines

```
from pyControl.utility import *
from devices import *

# Define hardware

button = Digital_input('X1', rising_event='button_press')
LED = Digital_output('X2')

# States and events.

states = ['LED_on',
         'LED_off']

events = ['button_press']

initial_state = 'LED_off'

# Variables

v.press_n = 0

# State behaviour functions.

def LED_off(event):
    if event == 'button_press':
        v.press_n = v.press_n + 1
        if v.press_n == 3:
            goto_state('LED_on')

def LED_on(event):
    if event == 'entry':
        LED.on()
        timed_goto_state('LED_off', 1*second)
        v.press_n = 0
    elif event == 'exit':
        LED.off()
```

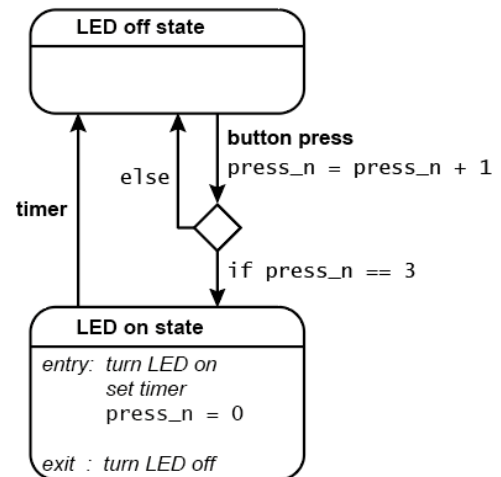


**Figure 1. Example task.** Complete task definition code (left panel) and corresponding state diagram (right panel) for a simple task that turns an LED on for 1 second when a button is pressed three times.

104 how the task responds to events. Events may be generated externally, for example by the  
105 subject's actions, or internally by timers.

106 Figure 1 shows the complete task definition code and the corresponding state diagram for a  
107 simple task in which pressing a button 3 times turns on an LED for 1 second. The code first  
108 defines the hardware that will be used, lists the task's state and event names, specifies the  
109 initial state, and initialises task variables.

110 The code then specifies task behaviour by defining a *state behaviour function* for each state.  
111 Whenever an event occurs, the state behaviour function for the current state is called with the  
112 event name as an argument. Special events called *entry* and *exit* occur when a state is  
113 entered and exited allowing actions to be performed on state transitions. State behaviour  
114 functions typically comprise a set of *if* and *else if* statements that determine what happens  
115 when different events occur in that state. Any valid Micropython code can be placed in a state  
116 behaviour function, the only constraint being that it must execute fast as it will block further  
117 state machine behaviour while executing. Users can define additional functions and classes  
118 in the task definition file that can be called from state behaviour functions. For example, code

119 implementing a reversal learning task's block structure might be separated from the state  
120 machine code in a separate function, improving readability and maintainability.

121 As should be clear from the above, while pyControl makes it easy to specify state machines,  
122 tasks are not strict finite state machines - in which the response to an event depends *only* on  
123 the current state, but rather extended state machines in which variables and arbitrary code  
124 can also determine behaviour.

125 We think this represents a good compromise between enforcing a specific structure on task  
126 code – which promotes readability and reliability and allows generic functionality to be  
127 efficiently implemented by the framework, while allowing users enough flexibility to compactly  
128 define a diverse range of complex tasks.

129 A key framework component is the ability to set timers to trigger state transitions or events.  
130 The *timed\_goto\_state* function, used in the example, triggers a transition to a specified state  
131 after a specified delay. Other functions allow timers to trigger a specified event after a  
132 specified delay, or to cancel, pause and un-pause timers that have already been set.

133 To make things happen in parallel with the main state set of the task, the user can define an  
134 *all\_states* function which is called, with the event name as an argument, whenever an event  
135 occurs irrespective of the state the task is in. This can be used in combination with timers and  
136 variables to implement task behaviour that occurs independently from or interacts with the  
137 main state set. For example to make something happen after a specified duration, irrespective  
138 of the current state, the user can set a timer to trigger an event after the required duration, and  
139 use the *all\_states* function to perform the required action whenever the event occurs.

140 pyControl provides a set of functions for generating random variables, and maths functions  
141 are available via the Micropython maths module. Though Micropython implements a large  
142 subset of the core Python language (see the [Micropython docs](#)), it is not possible to use  
143 packages such as *Numpy* or *Scipy* as they are too large to fit on a microcontroller.

#### 144 *Framework implementation*

145 The pyControl framework consists of approximately 1000 lines of Python code. Figure 2  
146 shows a simplified diagram of information flow between system components. Hardware inputs  
147 and elapsing timers place events in a queue where they await processing by the state  
148 machine. When events are processed, they are placed in a data output queue along with any  
149 state transitions and user print statements that they generate. This design allows different  
150 framework update processes to be prioritised by urgency, rather than by the order in which  
151 they become necessary, ensuring the framework responds at low latency even under heavy  
152 load (see validation experiments below). Top priority is given to processing hardware

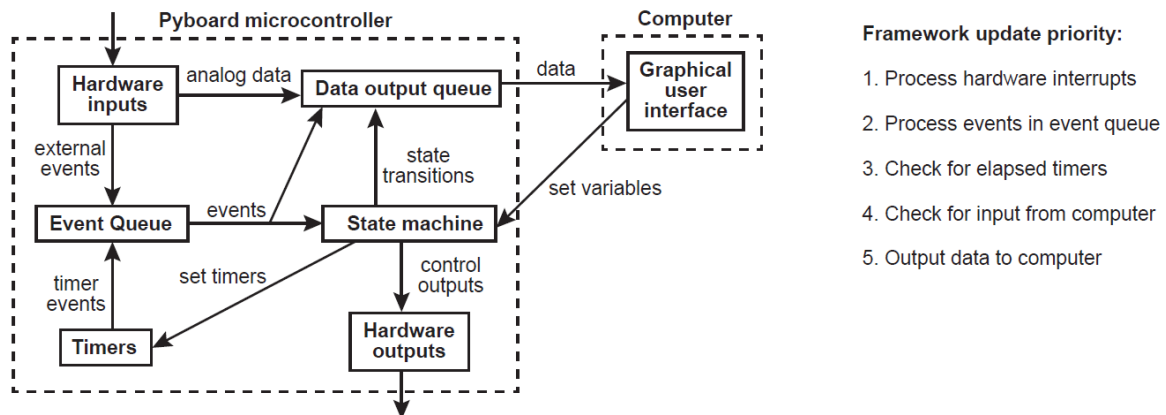


**Figure 2. Framework diagram.** Diagram showing the flow of information between different components of the framework and the GUI while a task is running. Right panel shows the priority with which processes occur in the framework update loop.

153 interrupts, secondary priority to passing events from the event queue to the state machine and  
154 processing their consequences, lowest priority to sending and receiving data from the  
155 computer.

156 Digital inputs are detected by hardware interrupts and can be configured to generate separate  
157 framework events on rising and falling edges. Analog inputs can stream continuous data to  
158 the computer and trigger framework events when the signal goes above and/or below a  
159 specified threshold.

## 160 *Hardware*

161 A typical pyControl hardware setup consists of a computer running the GUI, connected via  
162 USB to one or more breakout boards, each of which controls a single behavioural setup  
163 (Figure 3A). As task code runs on the microcontroller, the computer does not need to be  
164 powerful, we often use standard office desktops. We have not systematically tested the  
165 maximum number of setups that can be controlled from one computer but have run 24 in  
166 parallel without issue.

167 The breakout board interfaces a pyboard microcontroller with a set of *behaviour ports* used to  
168 connect devices that make up behavioural setups, as well as BNC connectors, indicator LEDs  
169 and user pushbuttons (Figure 3B). Each port is an RJ45 connector (compatible with standard  
170 network cables) with power lines (ground, 5V, 12V), two digital inputs/output (DIO) lines that  
171 are directly connected to microcontroller pins, and two driver lines for switching higher current  
172 loads. The driver lines are low side drivers (i.e. they connect the negative side of the load to  
173 ground) that can switch currents up to 150mA at voltages up to 12V, with clamp diodes to the  
174 12V rail to support inductive loads such as solenoids. Two ports have an additional driver line  
175 and two have an additional DIO. Six of the behaviour port DIO lines can alternatively be used

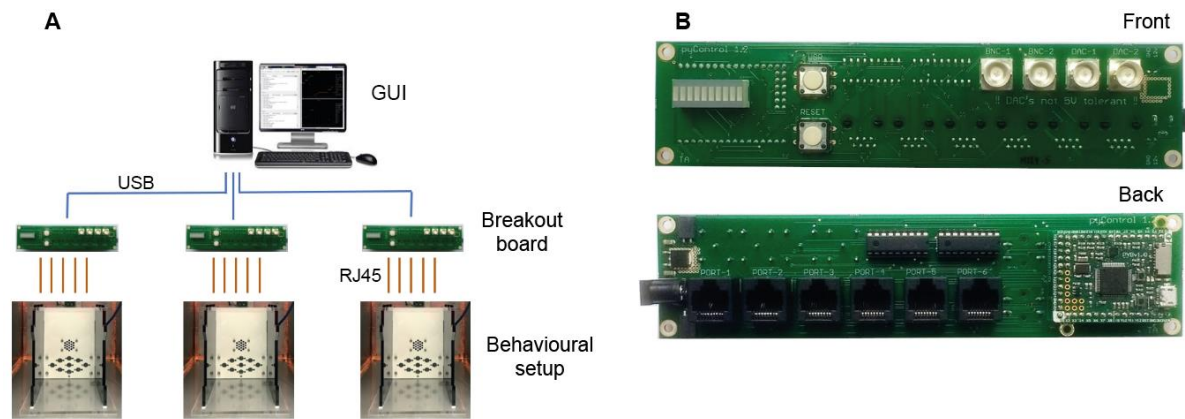


**Figure 3. pyControl hardware.** **A)** Diagram of a typical pyControl hardware setup, a single computer connects to multiple breakout boards, each of which controls one behavioural setup. Each behavioural setup is comprised of devices connected to the breakout board RJ45 behaviour ports using standard network cables. **B)** Breakout board interfacing the pyboard microcontroller with a set of behaviour ports, BNC connectors, indicator LEDs and user buttons. See supplementary figures S1-3 for hardware configurations used in the behavioural experiments reported in this manuscript, along with their associated hardware definition files. For more information see the [hardware docs](#).

176 as analog inputs and two as analog outputs. Three ports support UART and two support I2C  
177 serial communication over their DIO lines.

178 A variety of devices have been developed that connect to the ports, including nose-pokes,  
179 levers, audio boards, rotary encoders, stepper motor drivers, lickometers and LED drivers  
180 (Figures S1-3). Each has its own driver file that defines a Python class for controlling the  
181 device. For details see the [hardware docs](#). In addition to electronic devices, the hardware  
182 repository contains open source designs for operant boxes and sound attenuating chambers.  
183 It is straightforward for users to develop and share their own pyControl compatible devices,  
184 thanks to the documented behaviour port standard, and as device driver files are written in  
185 Python, and typically short and simple. For example the Karpova lab have independently  
186 developed and open sourced several pyControl compatible devices ([Github](#)).

187 Though it is possible to specify the hardware that will be used directly in a task file as shown  
188 in figure 1, it is typically done in a separate hardware definition file that is imported by the task.  
189 This avoids redundancy when many tasks are run on the same setup. Additionally, abstracting  
190 devices used in a task from the specific pins/ports they are connected to, allows the same task  
191 to run on different setups as long as their hardware definitions instantiate the required devices.  
192 See figures S1-3 for hardware definitions and corresponding hardware diagrams for the  
193 example applications detailed below.

194 For neuroscience applications, straightforward and failsafe synchronisation between  
195 behavioural data and other hardware such as cameras or physiology recordings is essential.  
196 pyControl implements a simple but robust method for this. Sync pulses are sent from

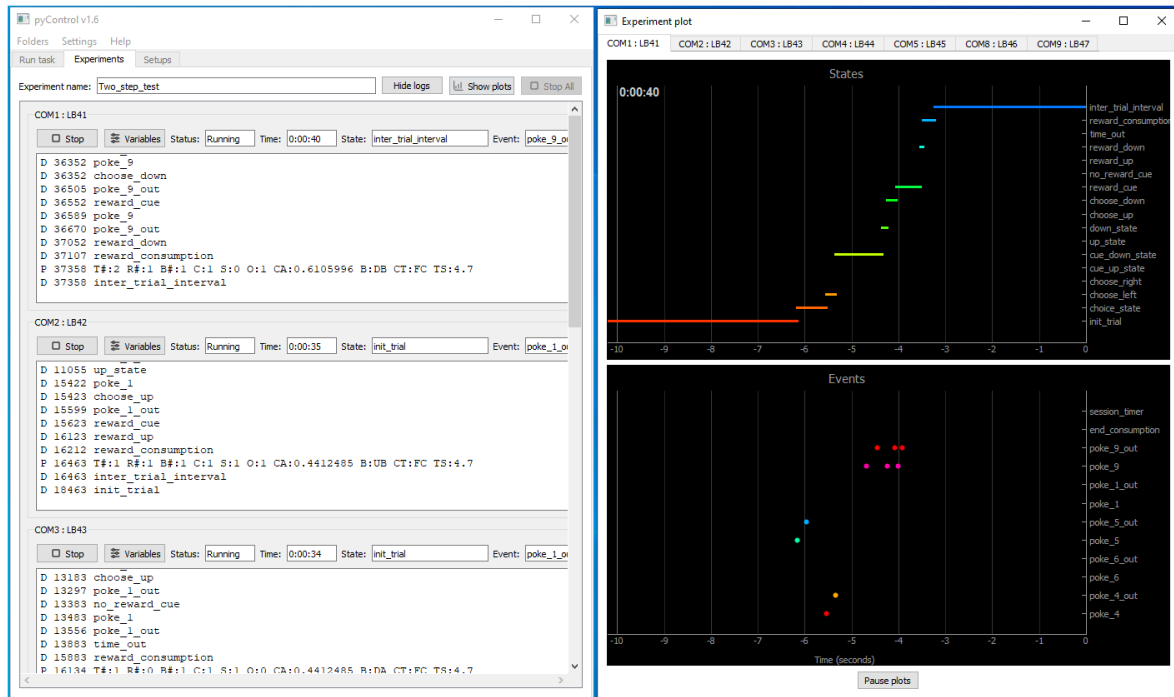


**Figure 4. pyControl GUI.** The GUI's *Experiments* tab is shown on the left running a multi-subject experiment, with the experiment's plot window open on the right showing the recent states and events for one subject. For images of the other GUI functionality see the [GUI docs](#).

197 pyControl to the other systems, which each record the pulse times in their own reference  
198 frame. The pulse train has random inter-pulse intervals which ensures a unique match  
199 between pulse sequences recorded on each system, so it is always possible to identify which  
200 pulse corresponds to which even if pulses are missing (e.g. due to forgetting to turn a system  
201 on until after the start of a session). This also makes it unambiguous whether two files come  
202 from the same session in the event of a file name mix-up. A Python module is provided for  
203 converting times between different systems using the sync pulse times recorded by each. For  
204 more information see the [synchronisation docs](#).

### 205 *Graphical User Interface*

206 The GUI provides two ways of setting up and running tasks; the *Run task* and *Experiments*  
207 tabs, as well as a *Setups* tab used to name and configure hardware setups.

208 The *Run task* tab allows the user to quickly upload and run a task on a single setup. It is  
209 typically used for prototyping tasks and testing hardware, but can also be used to acquire data.  
210 The values of task variables can be modified before the task is started or while the task is  
211 running. During the run, a log of events, state entries, and user print statements is displayed,  
212 and the events, states, and any analog signals are plotted in scrolling plot panels.

213 The *Experiments* tab is used for running experiments on multiple setups in parallel, and is  
214 designed to facilitate high-throughput experiments where multiple users run cohorts of animals



215 through a set of boxes. The user sets up the experiment by specifying which subjects will run  
216 on which setups, and the values of any variables that will be modified before the task starts.  
217 Experiment configurations can be saved and subsequently loaded. Variables can be set to  
218 the same value for all subjects or for individual subjects. Variables can be specified as  
219 *Persistent*, causing their value to be stored on the computer at the end of the session, and  
220 subsequently set to the same value the next time the experiment is run. Variables can be  
221 specified as *Summary*, causing their values to be displayed in a table at the end of the  
222 framework run and copied to the clipboard in a format that can be pasted directly into a  
223 spreadsheet, for example to record the number of trials and rewards for each subject.

224 When the experiment is run, a log of events, state entries, and user print statements is  
225 displayed for each subject, along with the current state, and most recent event and print  
226 statement (Figure 3). Variable values can be viewed and modified for individual subjects while  
227 the experiment is running. A tabbed plot window can be opened showing live scrolling plots  
228 of the events, states and analog signals for each subject, and individual subjects' plots can be  
229 undocked to allow behaviour of multiple subjects to be visualised simultaneously.

230 The GUI is implemented entirely in Python using the PyQt GUI framework and PyQtGraph  
231 plotting library. The code is organised into modules for communication with the pyboard,  
232 different GUI components, and data visualisation.

### 233 *pyControl data*

234 Data from pyControl sessions are saved as text files. When a session starts, information  
235 including the subject, task and experiment names, and start data and time, are written to the  
236 data file. While the task is running, all events and state transitions are saved automatically  
237 with millisecond timestamps. The user can output additional data by using the *print* function  
238 in their task file. This outputs the printed line to the computer, where it is displayed in the log  
239 and saved to the data file, along with a timestamp. In decision making tasks, we typically print  
240 one line each trial indicating the trial number, the subject's choice and trial outcome, along  
241 with any other relevant task variables. If an error occurs while the framework is running, a  
242 traceback reporting the error and line number in the task file where it occurred is displayed in  
243 the log and written to the data file. Continuous data from analog inputs is saved in separate  
244 binary files.

245 In addition to data files, task definition files used to generate data are copied to the  
246 experiment's data folder, with a file hash appended to the file name that is also recorded in  
247 the corresponding session's data file. This ensures that every task file version used in an  
248 experiment is automatically saved with the data, and it is always possible to uniquely identify  
249 the specific task file used for a particular session. If any variables are changed from default

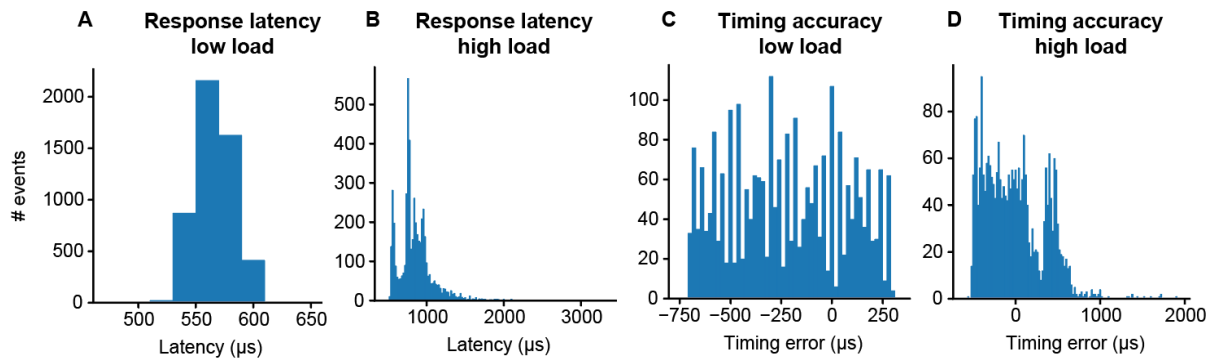


**Figure 5. Framework Performance.** **A)** Distribution of latencies for the pyControl framework to respond to a change in a digital input by changing the level of a digital output. **B)** As **A)** but under a high load condition (see main text). **C)** Distribution of pulse duration errors when framework generates a 10ms pulse. **D)** As **C)** but under a high load condition.

250 values in the task file this is automatically recorded in the session's data file. These automatic  
251 self-documenting features are designed to promote replicability of pyControl experiments. We  
252 encourage users to treat the versioned task files as part of the experiment's data and include  
253 them in data repositories.

254 Modules are provided for importing data files into Python for analysis and for visualising  
255 sessions offline. For more information see the [data docs](#).

### 256 Framework Performance:

257 To validate the performance of the pyControl framework we measured the system's response  
258 latency and timing accuracy. Response latency was assessed using a task which set a digital  
259 output to match the state of a digital input driven by a square wave signal. We recorded the  
260 input and output signals and plot the distribution of latencies between the two signals across  
261 all rising and falling edges (Figure 5A,B). In a 'low load' condition where the pyboard was not  
262 processing other inputs, response latency was  $556 \pm 17 \mu\text{s}$  (mean  $\pm$  SD). This latency reflects  
263 the time to detect the change in the input, trigger a state transition, and update the output  
264 during processing of the 'entry' event in the new state. We also measured response latency  
265 in a 'high load' condition where the pyboard was additionally monitoring two digital inputs each  
266 generating framework events in response to edges occurring as Poisson processes with an  
267 average rate of 200 Hz, and acquiring signal from two analog inputs at 1 kHz sample rate  
268 each. In this high load condition, the response latency was  $859 \pm 241 \mu\text{s}$  (mean  $\pm$  SD), the  
269 longest latency recorded was 3.3 ms with 99.6% of latencies <2 ms.

270 To assess timing accuracy, we used a task which turned on a digital output for 10 ms when a  
271 rising edge was received on a digital input. The input was driven by a 51 Hz square wave to  
272 ensure that the timing of input edges drifted relative to the framework's 1ms clock ticks. We  
273 plot the distribution of errors between the measured durations of the output pulses and the

274 10ms target duration (Figure 5C,D). In the low load condition, timing errors were  
275 approximately uniformly distributed across 1 ms (mean error -220  $\mu$ s, SD 282  $\mu$ s), as expected  
276 given the 1ms resolution of the pyControl framework clock ticks. In the high load condition,  
277 timing variability was only slightly increased (mean -10  $\mu$ s, SD 353  $\mu$ s), with the largest  
278 recorded error 1.9 ms and 99.5% of errors <1 ms. Overall, these data show that the  
279 framework's latency and timing accuracy are sufficient for the great majority of neuroscience  
280 applications, even when operating under loads substantially higher than experienced in typical  
281 tasks.

282 Users who require very tight timing/latency performance should be aware of Micropython's  
283 automatic garbage collection. Garbage collection is triggered when needed to free up memory  
284 and can take a couple of milliseconds. Input events or elapsing timers that occur during  
285 garbage collection will be processed once it has completed. To avoid garbage collection  
286 affecting time critical processes, the user can manually trigger garbage collection at a time  
287 when it will not cause problems (see [Micropython docs](#)), for example during the inter-trial  
288 interval. In the above validation experiments, garbage collection was triggered by the task  
289 code at a point in the task where it did not affect the measurements.

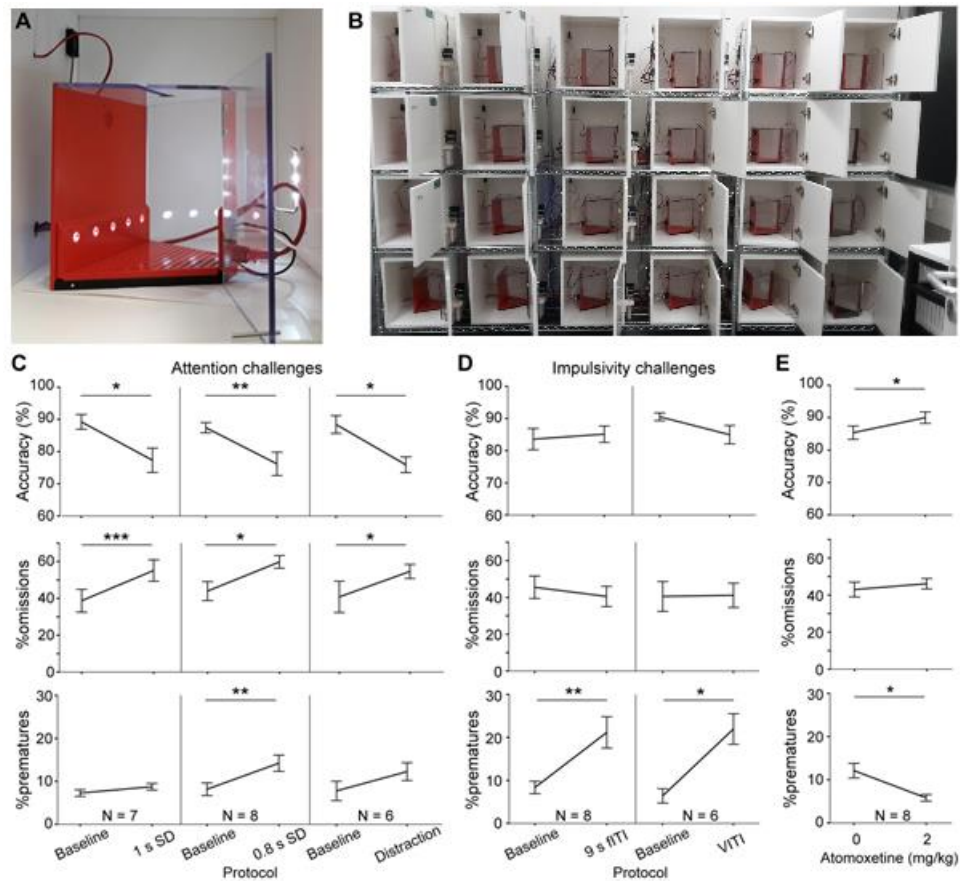
### 290 **Application examples:**

291 We illustrate how pyControl is used in practice with example applications in operant box, head-  
292 fixed and maze-based tasks. Task and hardware definition files for these experiments are  
293 provided in the manuscripts data repository. For additional use cases see the following studies  
294 (Korn et al., 2019; Akam et al., 2020; Koralek and Costa, 2020; Nelson et al., 2020).

#### 295 *5-choice serial reaction time task (5-CSRT)*

296 The 5-CSRT is a longstanding and widely used assay for measuring sustained visual attention  
297 and motor impulsivity in rodents (Carli et al., 1983; Bari et al., 2008). The subject must detect  
298 a brief flash of light presented pseudorandomly in one of five nose-poke ports, and report the  
299 stimulus location by poking the port, to trigger a reward delivered to a receptacle on the  
300 opposite wall.

301 We developed a custom operant box for the 5-CSRT (Figure 6 A,B), discussed in detail in a  
302 separate manuscript (Kapaniah, Akam. Kätzel et al. in prep). The pyControl hardware  
303 comprised a breakout board connected to a 5-poke board, which integrates the IR beams and  
304 stimulus LEDs for the 5 choice ports on a single PCB, a single poke board for the reward  
305 receptacle, an audio board, and a stepper motor board to control a peristaltic pump for reward  
306 delivery (Figure S1).



307 To validate the setup, a cohort of 8 C57BL/6 mice was trained in the 5-CSRTT using a staged  
308 training procedure (see Methods). The baseline protocol reached at the end of training used  
309 a stimulus duration (SD) of 2 s and a 5 s inter-trial interval (ITI) from the end of reward  
310 consumption to the presentation of the next stimulus. These task parameters were then  
311 manipulated to challenge subject's ability to either maintain sustained attention, or withhold  
312 impulsive premature responses. Attention was challenged in three conditions: by decreasing  
313 the SD to either 1 s or 0.8 s, or by an auditory distraction of 70 dB white noise, played between  
314 0.5 s and 4.5 s of the 5 s ITI. In all three attention challenges, the accuracy with which subjects

315 selected the correct port – the primary measure of sustained attention – decreased ( $P < 0.05$ ;  
316 paired t-tests comparing accuracy under the prior baseline protocol to accuracy under the  
317 challenge condition, Figure 6C). Also, as expected, omissions (i.e. failures to poke any port in  
318 the response window) increased ( $P < 0.05$ , t-test). In the attention challenges, the rate of  
319 premature responses - the primary measure of impulsivity, remained either unchanged (1 s  
320 SD challenge, auditory distraction;  $P > 0.1$ , t-test) or changed to a comparatively small extent  
321 (0.8 s SD challenge,  $P < 0.01$ , t-test). Similarly, when impulsivity was challenged by extending  
322 the ITI, to either a 9 s fixed ITI (fITI) or to a pseudo-randomly varied ITI length (vITI), premature  
323 responses increased strongly ( $P < 0.05$ , t-test), while attentional accuracy and omissions did  
324 not (Figure 6D). This specificity of effects of the challenges was as good – if not better – than  
325 that achieved by us previously in a commercial set-up (Med Associates, Inc.) (Grimm et al.,  
326 2018).

327 We further validated the task implementation by replicating effects of a pharmacological  
328 treatment – atomoxetine - that has been shown to reduce impulsivity in the 5-CSRTT (Navarra  
329 et al., 2008; Paterson et al., 2011). Using the 9 s fITI impulsivity challenge, we found that 2  
330 mg/kg atomoxetine could reliably reduce premature responding and increase attentional  
331 accuracy ( $P < 0.05$ , paired t-test comparing performance under vehicle vs. atomoxetine;  
332 Figure 6E), consistent with its previously described effect in this rodent task (Navarra et al.,  
333 2008; Paterson et al., 2011; Pillidge et al., 2014; Fitzpatrick and Andreasen, 2019).

#### 334 *Vibrissae-based object localisation task:*

335 We illustrate pyControl's utility for head-fixed behaviours with a version of the vibrissae-based  
336 object localisation task (O'Connor et al., 2010). Head-fixed mice used their vibrissae  
337 (whiskers) to discriminate the position of a pole moved into the whisker field at one of two  
338 different anterior-posterior locations (Figure 7A). The anterior 'Go' location indicated that  
339 licking in a response window after stimulus presentation would deliver a water reward, while  
340 the posterior 'NoGo' location indicated that licking in the response window would trigger a  
341 timeout (Figure 7B). Unlike in the original task mice were positioned on a treadmill allowing  
342 them to run. Although running was not required to perform the task, we observed 10-20 s  
343 running bouts alternated with longer stationary periods (Figure 7C), in line with previous  
344 reports (Ayaz et al., 2019). pyControl hardware used to implement the setup comprised a  
345 breakout board, a stepper motor driver to control the anterior-posterior position of the stimulus,  
346 a lickometer, and a rotary encoder to measure running speed (Figure S2).

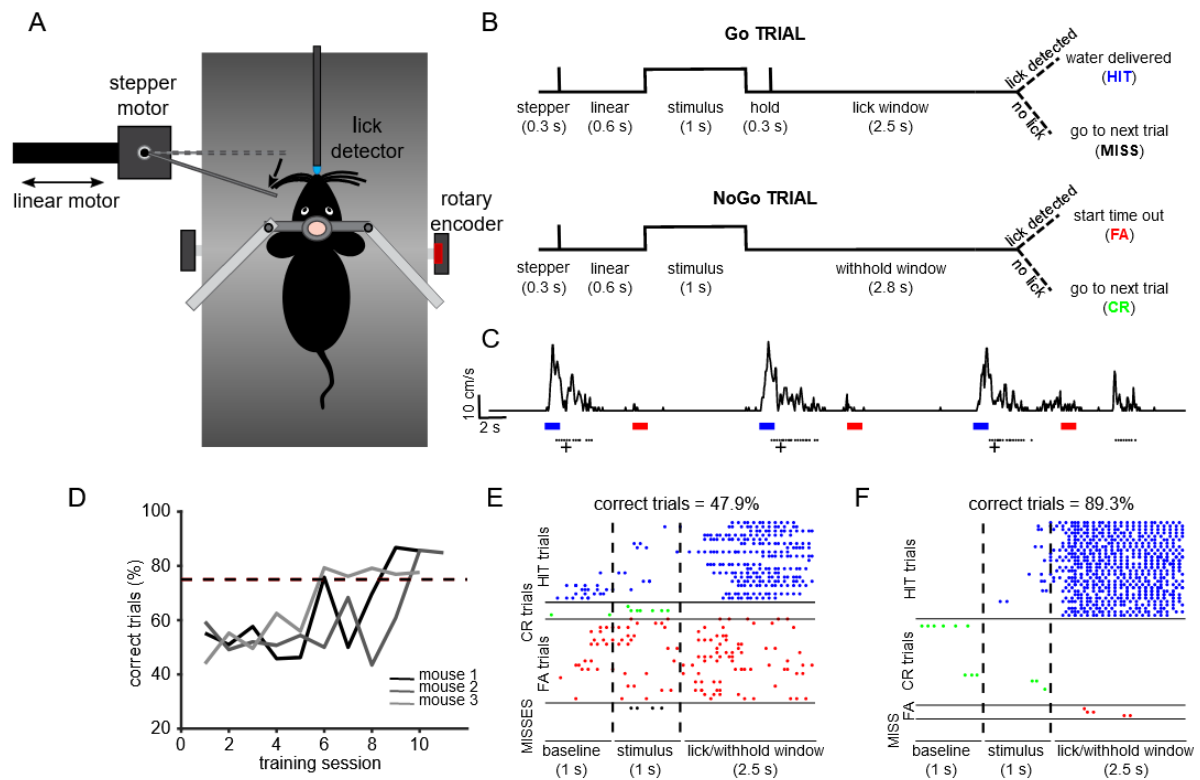


**Figure 7. Vibrissae-based object localisation task.** **A)** Diagram of the behavioural set up. Head-fixed mice were positioned on a treadmill with their running speed monitored by a rotary encoder. A pole was moved into the whisker field by a linear motor, with the anterior-posterior location controlled using a stepper motor. Water rewards were delivered via a spout positioned in front of the animal and licks to the spout were detected using an electrical lickometer. **B)** Trial structure: before stimulus presentation, the stepper motor moved into the trial position (anterior or posterior). Next, the linear motor translated the stepper motor and the attached pole close to the mouse’s whisker pad, starting the stimulation period. A lick window (during Go trials), or withhold window (during NoGo trials) started after the pole was withdrawn. FA = false alarm; CR = correct rejection. **C)** pyControl simultaneously recorded running speed (top trace) and licks (black dots) of the animals, as well as controlling stimulus presentation (blue and red bars for Go and NoGo stimuli) and solenoid opening (black crosses). **D)** Percentage of correct trials for 3 mice over the training period. Mice were considered expert on the task after reaching 75% correct trials (dotted line) and maintaining such performance for 3 consecutive days. **E)** Detected licks before, during and after tactile stimulation, during an early session before the mouse has learned the task, sorted by trial type: HIT trials (blue), CORRECT REJECTION trials (green), FALSE ALARMS trials (red), and MISS trials (black). Each row is a trial, each dot is a detected lick. Correct trials for this session were 47.9% of total trials. **F)** As **E)** but for data from the same mouse after reaching the learning threshold (correct trials = 89.3% of total trials).

347 Mice were first familiarised with the experimental setup by head-fixing them on the treadmill  
 348 for increasingly long periods of time (5-20 min) over three days. From the fourth day, mice  
 349 underwent a “detection training”, during which the pole was only presented in the Go position,  
 350 and water automatically delivered after each stimulus presentation. We then progressively  
 351 introduced NoGo trials, and made water delivery contingent on the detection of one or more

352 licks in the response window. Subjects reached 75% correct performance within five to nine  
353 days from the first training session, at which point, they were trained for at least three further  
354 days to make sure that they had reliably learned the task (Figure 7D). Early in training, mice  
355 frequently licked prior to and during stimulus presentation, as well as during the response  
356 window, on both Go and NoGo trials (Figure 7E). Following learning, licking prior to and during  
357 stimulus presentation was greatly reduced, and mice licked robustly during the response  
358 window on Go trials and withheld licking on NoGo trials, performing a high percentage of Hit  
359 and Correct Rejection trials (Figure 7F).

#### 360 *Social decision-making task:*

361 Our final application example is a maze-based social decision making task for mice, adapted  
362 from that developed for rats by Márquez et al. (2015). In this task a 'focal' animal's choices  
363 determine reward delivery for a 'recipient' animal, allowing preference for 'prosocial' vs 'selfish'  
364 choices to be examined. The behavioural apparatus comprised an automated double T-maze  
365 (Figure S3). Each T-maze consisted of a central corridor with nose-poke ports on each side  
366 (choice area) and two side arms each with a food receptacle connected to a pellet dispenser  
367 at the end (Figure 8A,B). Access from the central choice area to the side arms was controlled  
368 by pneumatic doors.

369 The task comprised two separate stages: (1) Individual training; where animals learn to open  
370 doors by poking the ports in the central arms and retrieve pellets in the side arms. (2) Social  
371 testing; where the decisions of the focal animal control the doors in both mazes, and hence  
372 determine rewards for both itself and the recipient animal in the other maze.

373 The individual training protocols were different for the focal and recipient animals. During  
374 individual training for the focal animal, a single poke in either port in the central arm opened  
375 the corresponding door, allowing access to a side arm. Accessing either side arm was  
376 rewarded with a pellet at the food receptacle in the arm. Under this schedule subjects  
377 increased their rate of completing trials over 7 training days (Figure 8C, repeated measures  
378 ANOVA  $F(6,42)=12.566$   $p=0.000004$ ) without developing a bias for either side of the maze ( $P$   
379  $> 0.27$  for all animals, t-test). During individual training for the recipient animal, only one of  
380 the nose-poke ports in the central arm was active, and the number of pokes required to open  
381 the corresponding door increased over 13 days of training, with 4 pokes eventually required  
382 to access the side arm to obtain a pellet in the food receptacle. Under this schedule the  
383 recipient animals developed a strong preference for the active poke over the course of training  
384 (Figure 8D right panel, repeated measures ANOVA  $F(12,24)=3.908$   $p=0.002$ ), with  
385 approximately 95% of pokes directed to the active side by the end of training.

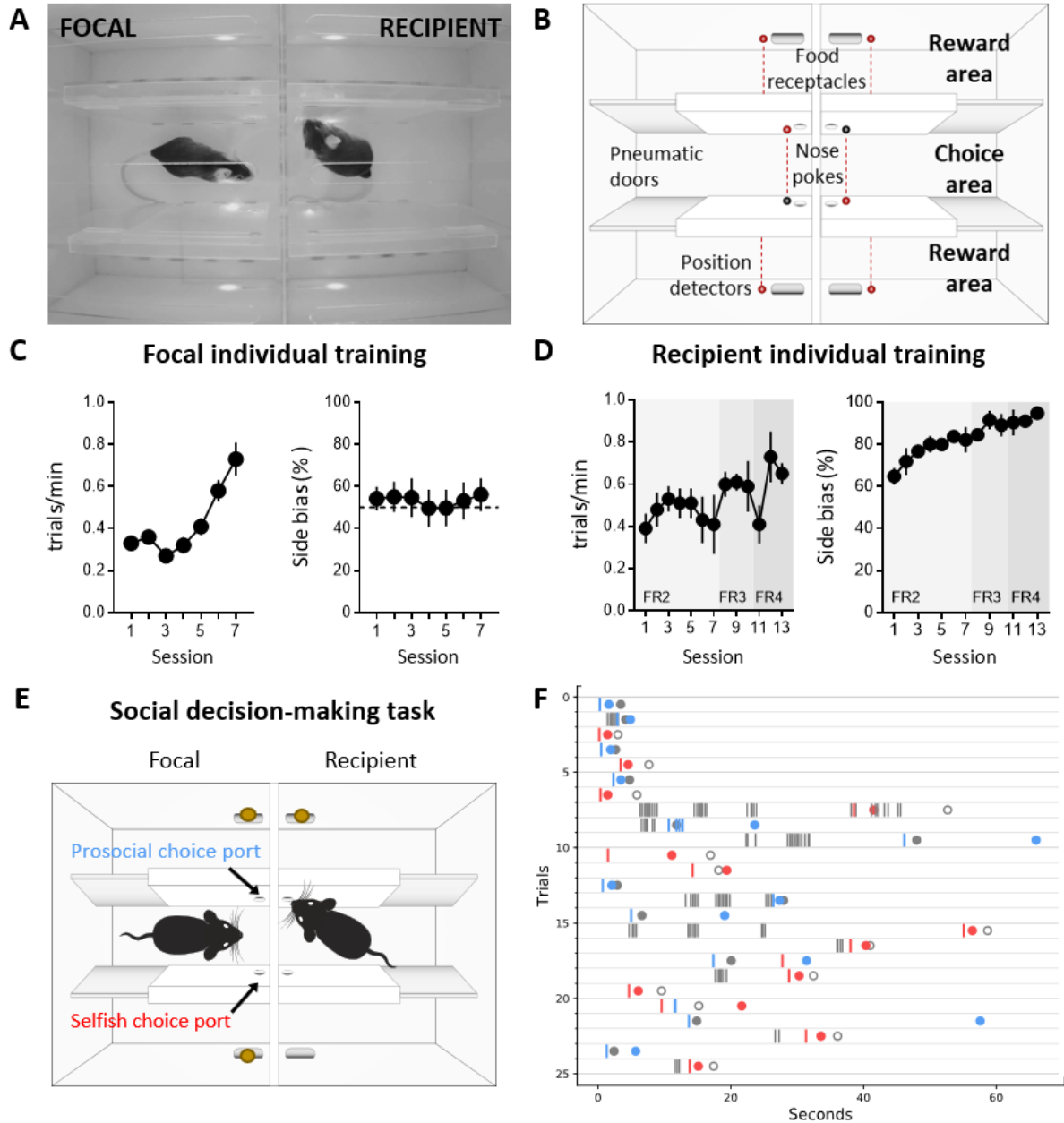


**Figure 8. Social decision making task.** **A)** Top view of double T maze apparatus showing two animals interacting during social decision making. **B)** Setup diagram; In each T maze, nose pokes are positioned on either side of the central choice area. Sliding pneumatic doors give access to the side arms of each maze (top and bottom in diagram) where pellet dispensers deliver food rewards. Six IR beams (depicted as grey and red circles connected by a dotted red line) detect the position of the animals to safely close the doors once access to an arm is secured. **C)** Focal animal individual training showing the number of trials completed per minute (left panel) and side bias (right panel) across days of training. **D)** As **C)** but for the recipient animal. **E)** Social decision making task. The trial starts with both animals in the central arm. The recipient animal has learnt in previous individual training to poke the port on the upper side of the diagram to give access to a food pellet in the corresponding reward area. During the social task the recipient animal's ports no longer control the doors but the animal can display food seeking behaviour by repeatedly poking the previously trained port. The focal animal has previously learned in individual training to collect food from the reward areas on both sides (top and bottom of diagram) by poking the corresponding port in the central choice area to activate the doors. During social decision making, the focal animal can either choose the 'prosocial' port, giving both animals access to the side (upper on diagram) of their respective



mazes where both receive reward, or can choose the 'selfish' port, giving both animals access to the other side (lower on diagram) where only the focal animal receives reward. **F)** Raster plot showing behaviour of a pair of animals over one session during early social testing. Nose pokes are represented by vertical lines, and colour coded according to the role of each mouse and choice type (grey – recipient's pokes, which are always directed towards the prosocial side, blue – focal's pokes in the prosocial choice port, red – focal's pokes in selfish port). Note that latency for focal choice varies depending on the trial, allowing the recipient to display its food seeking behaviour or not. Circles indicate the moment where each animal visits the food-receptacle in their reward arm. Focal animals are always rewarded, and the colour of the filled circle indicates the type of trial after decision (blue – prosocial choice, red – selfish choice). Grey circles indicate time of receptacle visit for recipients, where filled circles correspond to prosocial trials, where recipient is also rewarded, and open circles to selfish trials, where no pellet is delivered.

---

386 During social testing, the two animals were placed in the double T-maze, one in each T,  
387 separated by a transparent perforated partition that allowed the animals to interact using all  
388 sensory modalities. The doors in the recipient animal's maze were no longer controlled by the  
389 recipient animal's pokes, but were rather yoked to the doors of the focal animal, such that a  
390 single poke to either port in the focal animals choice area opened the doors in both mazes on  
391 the corresponding side. As in individual training, the focal animal was rewarded for accessing  
392 either side, while the recipient animal was rewarded only when it accessed one side of the  
393 maze. The choice made by the focal animal therefore determined whether the recipient animal  
394 received reward, so the focal animal could either make 'pro-social' choices which rewarded  
395 both it and the recipient, or 'selfish' choices which rewarded only the focal animal. As a proof  
396 of concept, we show nose pokes and reward deliveries from a pair of interacting mice from  
397 one social session (Figure 8F). A full analysis of the social behaviour in this task will be  
398 published separately (Esteve-Agraz and Marquez, in preparation).

## 399 Discussion

400 pyControl is an open source system for running behavioural experiments, whose principal  
401 strengths are: 1. a flexible and intuitive Python based syntax for programming tasks. 2.  
402 Inexpensive, simple and extensible behavioural hardware that can be purchased commercially  
403 or assembled by the user. 3. A GUI designed for efficiently running high throughput  
404 experiments on many setups in parallel from a single computer. 4. Extensive online  
405 documentation and user support.

406 pyControl can contribute to behavioural neuroscience in two important ways: First, it makes it  
407 quicker, easier and cheaper to implement a wide range of behavioural tasks and run them at  
408 scale. Second, it facilitates communication and reproducibility of behavioural experiments,  
409 both because the task definition syntax is highly readable, and because self-documenting  
410 features ensure that the exact task version and parameters used to generate data are  
411 automatically stored with the data itself.

412 pyControl's strengths and limitations stem from underlying design choices. We will discuss  
413 these primarily in relation to two widely used open source systems for experiment control in  
414 neuroscience [Bpod](#) (Josh Sanders) and [Bonsai](#) (Lopes et al., 2015). Bpod is a useful point  
415 of comparison as it is probably the most similar project to pyControl in terms of functionality  
416 and implementation, Bonsai because it represents a very different but powerful formalism for  
417 controlling experiments that is often complementary. Space constraints preclude detailed  
418 comparison with other projects, but see (Devarakonda et al., 2016; O'Leary et al., 2018; Kim  
419 et al., 2019; Gurley, 2019; Bhagat et al., 2020; Buscher et al., 2020).

420 Both pyControl and Bpod provide a state-machine-based task definition syntax in a high-level  
421 programming language, run the state machine on a microcontroller, have commercially  
422 available open source hardware, graphical interfaces for controlling experiments, and are  
423 reasonably mature systems with a substantial user base beyond the original developers.  
424 Despite these commonalities, there are significant differences which it is useful for prospective  
425 users to understand.

426 The first is that in pyControl, user created task definition code runs directly on a pyboard  
427 microcontroller, supported by framework code that determines when user defined functions  
428 are called. This contrasts with Bpod, where user code written in either Matlab (Bpod) or  
429 Python (PyBpod) is translated into instructions passed to the microcontroller, which itself runs  
430 firmware implemented in the lower-level language C++. These two approaches offer distinct  
431 advantages and disadvantages.

432 Running user Python code directly on the microcontroller avoids separating the task logic into  
433 two conceptually distinct levels – flexible code written in a high-level language that runs on the  
434 computer, and the more constrained set of operations supported by the microcontroller  
435 firmware. Our understanding of how this works in Bpod is that the high level user code  
436 implements a loop over trials where each loop defines a finite state machine for the current  
437 trial - specifying for each state which outputs are on, and which events trigger transitions to  
438 which other states, then uploads this information to the microcontroller, runs the state machine  
439 until it reaches an exit condition indicating the end of the trial, and finally receives information  
440 from the microcontroller about what happened before starting the next trial's loop. The  
441 microcontroller firmware implements some functionality beyond a strict finite state machine  
442 formalism, including timers and event counters that are not tied to a particular state, but does  
443 not support arbitrary user code or variables. We suggest readers consult the relevant  
444 documentation ([pyControl](#), [Bpod](#), [PyBpod](#)) and example tasks ([pyControl](#), [Bpod](#), [pyBpod](#)) to  
445 compare syntaxes directly. A second advantage of running user code directly on the  
446 microcontroller is that the user has direct access from their task code to microcontroller

447 functionality such as serial communication. A third is that the pyControl framework (as well  
448 as the GUI) is written in Python rather than C++, facilitating code maintenance, and lowering  
449 the barrier to users extending system functionality.

450 The two principal disadvantages of running the task entirely on the microcontroller are: 1)  
451 although modern microcontrollers are very capable, their resources are more limited than a  
452 computer - which constrains how computationally and memory intensive task code can be and  
453 precludes using modules such as Numpy. 2) Lack of access to the computer from task code,  
454 for example to interact with other programs or display custom plots. To address these  
455 limitations, we are currently developing an application programming interface (API) to allow  
456 pyControl tasks running on the microcontroller to interact with user code running on the  
457 computer. This will work via the user defining a Python class with methods that get called at  
458 the start and end of the run for initial setup and post-run clean-up, as well as an update method  
459 called regularly during the run with any new data received from the board as an argument.

460 There are also differences in hardware design. The two most significant are; 1) The pyControl  
461 breakout board tries to make connectors (behaviour ports and BNC) as flexible as possible at  
462 the cost of not being specialised for particular functions. Bpod tends to use a given connector  
463 for a specific function - e.g. it has separate *behaviour ports* and *module ports*, with the former  
464 designed for controlling a nose-poke, and the latter for UART serial communication with  
465 external modules. Practically, this means that pyControl exposes microcontroller pins (which  
466 often support multiple functions) directly on connectors whereas Bpod tends to incorporate  
467 intervening circuitry such as electrical isolation for BNC connectors and serial line driver ICs  
468 on module ports. 2) Bpod uses external modules, each with its own microcontroller and C++  
469 firmware, for functions which pyControl implements using the microcontroller on the breakout  
470 board, specifically; analog input and output, I2C serial communication, and acquiring signal  
471 from a rotary encoder. These design choices make pyControl hardware simpler and cheaper.  
472 Purchased commercially the Bpod state machine costs \$765, compared to €250 for the  
473 pyControl breakout board, and Bpod external modules each cost hundreds of dollars. This is  
474 not to say that pyControl necessarily represent better value; a given Bpod module may offer  
475 more functionality (e.g. more channels, higher sample rates). But the two systems do  
476 represent different design approaches.

477 Both the pyControl and pyBpod GUI's support configuring and running experiments on multiple  
478 setups in parallel from a single computer, while the Matlab based Bpod GUI controls a single  
479 setup at a time. Their user interfaces are each very different, the respective user guides  
480 ([pyControl](#), [Bpod](#), [PyBpod](#)) give the best sense for the different approaches. We think it is a  
481 strength of the pyControl GUI, reflecting the relative simplicity of the underlying code base,

482 that scientist users not originally involved in the development effort have made substantial  
483 contributions to its functionality (see GitHub [pull requests](#)).

484 Bonsai (Lopes et al., 2015) represents a very different formalism for experiment control that is  
485 not based around state machines. Instead, the Bonsai user designs a *dataflow* by arranging  
486 and connecting nodes in a graphical interface, where nodes may represent data sources,  
487 processing steps, or outputs. Bonsai can work with a diverse range of data types including  
488 video, audio, analog and digital signals. Multiple data streams can be processed in parallel  
489 and combined via a rich set of operators including arbitrary user code. Bonsai is very powerful,  
490 and it is likely that any task implemented in pyControl could also be implemented in Bonsai.  
491 The reverse is certainly not true, as Bonsai can perform computationally demanding real time  
492 processing on high dimensional data such as video, which is not supported by pyControl.

493 Nonetheless, in applications where either system could be used, there are reasons why  
494 prospective users might consider pyControl: 1) pyControl's task definition syntax may be more  
495 intuitive for tasks where (extended) state machines are a natural formalism. The reverse is  
496 true for tasks requiring parallel processing of multiple complex data streams. 2) pyControl is  
497 explicitly designed for efficiently running high throughput experiments on many setups in  
498 parallel. Though it is possible to control multiple hardware setups from a single Bonsai  
499 dataflow, Bonsai does not explicitly implement the concept of a multi-setup experiment so the  
500 user must duplicate dataflow components for each setup themselves. As task parameters  
501 and data file names are specified across multiple nodes in the dataflow, configuring these for  
502 a cohort of subjects can be laborious - though it is possible to automate this by calling Bonsai's  
503 command line interface from user created Python scripts. 3) pyControl hardware modules can  
504 simplify the physical construction of behavioural setups. In practice, we think the two systems  
505 are often complementary, for example we use Bonsai in our workflow for acquiring and  
506 compressing video data from sets of pyControl operant boxes ([Github](#)), and we hope to  
507 integrate them more closely in future.

508 pyControl is under active development. We are currently prototyping a home-cage training  
509 system which integrates a pyControl operant box with a mouse home-cage, via an access  
510 control module which allows socially housed animals to individually access the operant box to  
511 train themselves with minimal user intervention. We are also developing hardware to enable  
512 much larger scale behavioural setups, such as complex maze environments with up to 68  
513 behaviour ports per setup. As discussed above, we are finalising an API to allow pyControl  
514 tasks to interact with user Python code running on the computer.

515 In summary, pyControl is a user friendly and flexible tool addressing a commonly encountered  
516 use case in behavioural neuroscience; defining behavioural tasks as extended state

517 machines, running them efficiently as high throughput experiments, and communicating task  
518 logic to other researchers.

519 **Acknowledgments:**

520 T.A. thanks current and former members of the Champalimaud hardware and software  
521 platforms; Jose Cruz, Ricardo Ribeiro, Carlos Mão de Ferro and Matthieu Pasquet for  
522 discussions and technical assistance, and Filipe Carvalho and Lídia Fortunato of Open Ephys  
523 Production Site for hardware assembly and distribution. C.M. thanks Victor Rodriguez for  
524 assistance developing the social decision making apparatus. M.P. and M.K. thank Dr Ana  
525 Carolina Bottura de Barros and Dr Severin Limal for assistance with the Vibrissae-based  
526 object localisation task.

527 T.A. was funded by was funded by Wellcome Trust grants WT096193AIA, 202831/Z/16/Z and  
528 214314/Z/18/Z M.E.W was funded by the Wellcome Trust grants 202831/Z/16/Z. A.L. was  
529 funded by the Howard Hughes Medical Institute. C.M. was funded by Ciencia e Innovación,  
530 Spain, under grant RTI2018-097843-B-100, the “Severo Ochoa” Program for Centers of  
531 Excellence in R&D (SEV-2013-0317 and SEV-2017-0723) and Ministerio de Ciencia e  
532 Innovación with a Ramon y Cajal contract (RYC-2014-16450). J.E-A was funded by the  
533 Generalitat Valenciana and European Union (ACIF/2019/017). D.K. was funded by the Else-  
534 Kröner-Fresenius-Foundation/German-Scholars-Organization (Programme for Excellent  
535 Medical Scientists from abroad; GSO/EKFS 12and the DFG (KA 4594/2-1). M.P. was funded  
536 by Wellcome Trust grant 109908/Z/15/Z and Human Frontiers Science Programme grant  
537 RGY0073/2015 to M.K. R.M.C. was funded by the National Institute of Health  
538 (5U19NS104649) and ERC CoG (617142).

539 **Author Contributions:**

540 Developed hardware: T.A. Developed software: T.A., A.L., J.R. Designed and ran behavioural  
541 experiments: S.K., J.E-A, M.P, C.M, M.K, D.K. Wrote the manuscript: T.A, S.K., J.E-A, M.P,  
542 C.M, M.K, D.K. Edited the manuscript: R.M.C., M.W.

543 **Competing Interests:**

544 T.A. has a consulting contract with Open Ephys Production Site who sell assembled pyControl  
545 hardware. The other authors have no competing interests to report.

546

547

548 **Methods:**

549 pyControl task files used in all experiments, and data and analysis code for the performance  
550 validation experiments, are included in the manuscript's [data and code repository](#).

551 *Framework performance validation*

552 Framework performance was characterised using pyboards running Micropython version 1.13  
553 and pyControl version 1.6. Electrical signals used to characterise response latency and timing  
554 accuracy (Figure 5) were recorded at 50 kHz using a Picoscope 2204A USB oscilloscope.

555 To assess response latency, a pyboard running the task file *input\_follower.py* received a 51  
556 Hz square wave input generate by the picoscope's waveform generator. The task turned an  
557 output on and off to match the state of the input signal. The latency distribution was assessed  
558 by recording 50 seconds of the input and output signals and evaluating the latency between  
559 the signals at each rising and falling edge.

560 To assess timing accuracy, a pyboard running the task file *triggered\_pulses.py* received a  
561 51Hz square wave input generate by the picoscope's waveform generator. The task triggered  
562 a 10ms output pulse whenever a rising edge occurred in the input signal. The output signals  
563 was recorded for 50 s and the duration of each output pulses was measured to assess the  
564 distribution of timing errors.

565 In both cases the experiments were performed separately in a low load and high load  
566 condition. In the low load condition the task was not monitoring any other inputs. In the high  
567 load condition, the task was additionally acquiring data from two analog inputs at 1 kHz sample  
568 rate each, and monitoring two digital inputs, each of which was generating framework events  
569 in response to edges occurring as a Poisson process with average rate 200 Hz. These  
570 Poisson input signals were generated by a second pyboard running the task  
571 *poisson\_generator.py*.

572 **Application examples**

573 *5 choice serial reaction time task:*

574 Animals

575 The 5-CSRTT experiment used a cohort of 8 male C57BL/6 mice, aged 3-4 months at the  
576 beginning of training. Animals were group-housed (2-3 mice per cage) in Type II-Long  
577 individually ventilated cages (Greenline, Tecniplast, G), enriched with sawdust, sizzle-nest<sup>TM</sup>,  
578 and cardboard houses (Datesand, UK), and subjected to a 13 h light / 11 h dark cycle. Mice  
579 were kept under food-restriction at 85-95% of their average free-feeding weight which was

580 measured over 3 d immediately prior to the start of food-restriction at the start of the  
581 behavioural training. Water was available ad libitum.

582 This experiment was performed in accordance to the German Animal Rights Law  
583 (Tierschutzgesetz) 2013 and approved by the Federal Ethical Review Committee  
584 (Regierungspräsidium Tübingen) of Baden-Württemberg.

585 Behavioural hardware

586 The design of the operant boxes for the 5-CSRTT setups will be discussed in detail in a  
587 separate manuscript (Kapaniah, Akam, Kätzel et al. in prep). Briefly, the box had a trapezoidal  
588 floorplan with the 5 choice wall at the wide end and reward receptacle at the narrow end of  
589 the trapezoid, to minimize the floor area and hence reduce distractions. The side-walls and  
590 roof were made of transparent acrylic to allow observation of the animal, the remaining walls  
591 were made from opaque PVC to minimize visual distractions (Figure 6a). Design files for the  
592 operant box, and peristaltic and syringe pumps for reward delivery, are at  
593 <https://github.com/KaetzelLab/Operant-Box-Design-Files>. Potentially distracting features  
594 (house light, cables) were located outside of the box and largely invisible from the inside. The  
595 pyControl hardware used and the associated hardware definition is shown in figure S1. The  
596 operant box was enclosed by a sound attenuating chamber, custom made in 20mm melamine-  
597 coated MDF, adapted from a design in the [hardware repository](#). The pyControl breakout  
598 boards, and other PCBs that were not integrated into the box itself, were mounted on the  
599 outside of the sound attenuating chamber, and a CCTV camera was mounted on the ceiling  
600 to monitor behavior.

601 5-CSRTT training

602 The 5-CSRTT training protocol was similar to what we described previously (Grimm et al.,  
603 2018). In brief, after initiation of food-restriction, mice were accustomed to the reward  
604 (strawberry milk, Müllermilch™, G) in their home cage and in the operant box (2-3 exposures  
605 each). Then, mice were trained on a simplified operant cycle in which all holes of the 5-poke  
606 wall were illuminated for an unlimited time, and the mouse could poke into any one of them to  
607 illuminate the reward receptacle on the opposite wall and dispense a 40  $\mu$ l milk reward. Once  
608 mice attained at least 30 rewards each in two consecutive sessions, they were moved to the  
609 5-CSRTT task.

610 During 5-CSRTT training, mice transitioned through five stages of increasing difficulty, based  
611 on reaching performance criteria in each stage (Table 1). The difficulty of each stage was  
612 determined by the length of time the stimulus was presented (stimulus duration, SD) and the

5-CSRTT training						
	Task Parameters		Criteria for stage transition (2 consecutive days)			
Stage	SD (s)	ITI (s)	# correct	% correct	% accuracy	% omissions
S1	20	2	>= 30	>= 40	-	-
S2	8	2	>= 40	>= 50	-	-
S3	8	5			>= 80	<= 50
S4	4	5			>= 80	<= 50
S5	2	5			>= 80	<= 50
Challenges						
C1	2	9	Impulsivity challenge			
C2	1	5	Attention challenge 1			
C3	0.8	5	Attention challenge 2			
C4	2	5	Distraction: 1s white noise within 0.5-4.5s of ITI			
C5	2	7, 9, 11, 13	Variable ITI: pseudo-random, equal distribution			

**Table 1. 5-CSRTT Training and challenge stages.** The parameters stimulus duration (SD) and intertrial-interval (ITI, waiting time before stimulus) are listed for each of the 5 training stages (S1-5) and the subsequent challenge protocols on which performance was tested for 1 day each (C1-5). For the training stages, performance criteria which had to be met by an animal on two consecutive days to move to the next stage are listed on the right. See Methods for the definition of these performance parameters.

613 length of the inter-trial interval (ITI) between the end of the previous trial and the stimulus  
614 presentation on the next trial.

615 The ITI was initiated when the subject exited the reward receptacle after collection of a reward,  
616 or by the end of a time-out period (see below). The ITI was followed by illumination of one hole  
617 on the 5-choice wall for the SD determined by the training stage. A poke in the correct port  
618 during the stimulus, or during a subsequent 2s hold period, was counted as a *correct*  
619 *response*, illuminating the reward receptacle and dispensing 20  $\mu$ l of milk. If the subject either  
620 poked into any hole during the ITI (*premature response*), poked into a non-illuminated hole  
621 during the SD or hold period (*incorrect response*), or failed to poke during the trial (*omission*),  
622 the trial was not rewarded but instead terminated with a 5 s time-out during which the house  
623 light was turned off. The relative numbers of each response type were used as performance  
624 indicators measuring premature responding [ $\%premature = 100 * (\text{number of premature responses}) / (\text{number of trials})$ ],  
625 sustained attention [ $accuracy = 100 * (\text{number of correct responses}) / (\text{number of correct and incorrect responses})$ ],  
626 and lack of participation [ $\%omissions = 100 * (\text{number of omissions}) / (\text{number of trials})$ ]. In all stages and tests, sessions  
627 lasted 30 min and were performed once daily at the same time of day.  
628

629 Test days with behavioural challenges were interleaved with at least one training day on the  
630 baseline stage (stage 5; see Table 1 for parameters of all stages). For pharmacological



631 validation, atomoxetine (Tomoxetine hydrochloride, Tocris, UK) diluted in sterile saline (0.2  
632 mg/ml) or saline vehicle were injected i.p. at 10  $\mu$ l/g mouse injection volume 30 min before  
633 testing started. For atomoxetine vs. vehicle within-subject comparison, two tests were  
634 conducted separated by one week, whereby four animals received atomoxetine on the first  
635 day, while the other four received vehicle and vice versa for the second day. Effects of  
636 challenges (compared to performance on the prior day with baseline training) and atomoxetine  
637 (compared to performance under vehicle) were assessed by paired-samples *t*-tests.

#### 638 *Vibrissae-based object localisation task:*

##### 639 Animals

640 Subjects were three female mice expressing the calcium-sensitive protein GCaMP6s in  
641 excitatory neurons, derived by mating the floxed Ai94(TITL-GCaMP6s)-D line (Jackson  
642 Laboratories; stock number 024742) with the CamKII-tta (Jackson Laboratories; stock number  
643 003010). Animal husbandry and experimental procedures were approved and conducted in  
644 accordance with the United Kingdom Animals (Scientific Procedures) Act 1986 under project  
645 license P8E8BBDAD and personal licenses from the Home Office.

##### 646 Behavioural hardware

647 Mice were head-fixed on a treadmill fashioned from a 24 cm diameter Styrofoam cylinder  
648 covered with 1.5 mm thick neoprene. An incremental optical encoder (Broadcom HEDS-  
649 5500#A02; RS Components) was used in conjunction with a pyControl rotary encoder adapter  
650 to monitor mouse running speed. The pole used for object detection was a blunt 18G needle  
651 mounted, via a 3d-printed arm, onto a stepper motor (RS PRO Hybrid 535-0467; RS  
652 Components). The stepper motor was mounted onto a motorized linear stage (DDSM100/M;  
653 Thorlabs) used to move the pole toward and away from the whisker pad (controlled by a K-  
654 Cube Brushless DC Servo Driver (KBD101; Thorlabs). The pyControl hardware used and the  
655 associated hardware definition is shown in figure S2.

##### 656 Surgery

657 6-10 week old mice were anaesthetised with isoflurane (0.8-1.2% in 1 L/min oxygen) and  
658 implanted with custom titanium headplates for head-fixation and 4 mm diameter cranial  
659 windows for imaging as described previously (Chong et al., 2019). Peri- and post-operative  
660 analgesia was used (meloxicam 5mg/kg and buprenorphine 0.1 mg/kg) and mice were  
661 carefully monitored for 7 days post-surgery.

662 Behavioural training

663 Following recovery from surgery, mice were habituated to head-fixation (Chong et al.,  
664 2019) prior to training on the vibrissa-based object localisation task as detailed in the results  
665 section.

666 *Social decision making task:*

667 Animals

668 12 male C57BL6/J mice (Charles River, France) were used, aged 3 months at the beginning  
669 of the experiment. Animals were group-housed (4 animals per cage) and maintained with ad  
670 libitum access to food and water in a 12 – 12 h reversed light cycle (lights off at 8 am) at the  
671 Animal Facility of the Instituto de Neurociencias of Alicante. Short food restrictions (2 h before  
672 the behavioural testing) were performed in the early phases of individual training to increase  
673 motivation for food-seeking behaviour, otherwise animals were tested with ab libitum chow  
674 available in their home cage. All experimental procedures were performed in compliance with  
675 institutional Spanish and European regulations, as approved by the Universidad Miguel  
676 Hernández Ethics committee.

677 Behavioural hardware

678 The Social decision making task was performed in a double maze, where two animals, the  
679 focal and the recipient, would interact and work to obtain food rewards. The outer walls of the  
680 double maze were of white laser cut acrylic. Each double maze was divided by a transparent  
681 and perforated wall creating the individual mazes for each mouse. For each individual maze,  
682 inner walls separating central choice and side reward areas, contained the mechanisms for  
683 sliding doors, 3D printed nose-pokes and position detectors. These inner walls were made of  
684 transparent laser cut acrylic, in order to allow visibility of the animal in the side arms of the  
685 maze. Walls of the central choice area were frosted to avoid reflections that could interfere  
686 with automated pose estimation of the interacting animals in this area.

687 Each double T-maze behavioural setup was positioned inside a custom-made sound isolation  
688 box, with an infra-red sensitive camera (PointGrey Flea3 -U3-13S2M CS, Canada) positioned  
689 above the maze to track the animals' location. The chamber was illuminated with dim white  
690 light (4 lux) and infra-red illumination located on the ceiling of the sound attenuating chamber.  
691 The pyControl hardware configuration and associated hardware definition file are shown in  
692 figure S3. Food pellet rewards were dispensed using pellet dispensers made of 3D printed  
693 and laser cut parts actuated by a stepper motor (NEMA 42HB34F08AB, e-ika electrónica y  
694 robótica, Spain) controlled by a pyControl stepper driver board, placed outside the sound

695 isolation box and delivering the pellets to the 3D printed food receptacles through a silicon  
696 tube. Design files for the pellet dispenser and receptacles are at  
697 <https://github.com/MarquezLab/Hardware>. The sliding doors that control access to the side  
698 arms were actuated by pneumatic cylinders (Cilindro ISO 6432, Vestonn Pneumatic, Spain)  
699 placed below the base of the maze, providing silent and smooth horizontal movement of the  
700 doors. These were in turn controlled via solenoid valves (8112005201, Vestonn Pneumatic,  
701 Spain) interfaced with pyControl using an optocoupled relay board (Cebek- T1, Fadisel,  
702 Spain). The speed of the opening/closing of the doors could be independently regulated by  
703 adjusting the pressure of the compressed air to the solenoid valves.

704 Behavioural training

705 Individual training and social decision making protocols are described in the results section.  
706 All behavioural experiments and were performed during the first half of the dark phase of the  
707 cycle.

708

709

710

711 **References**

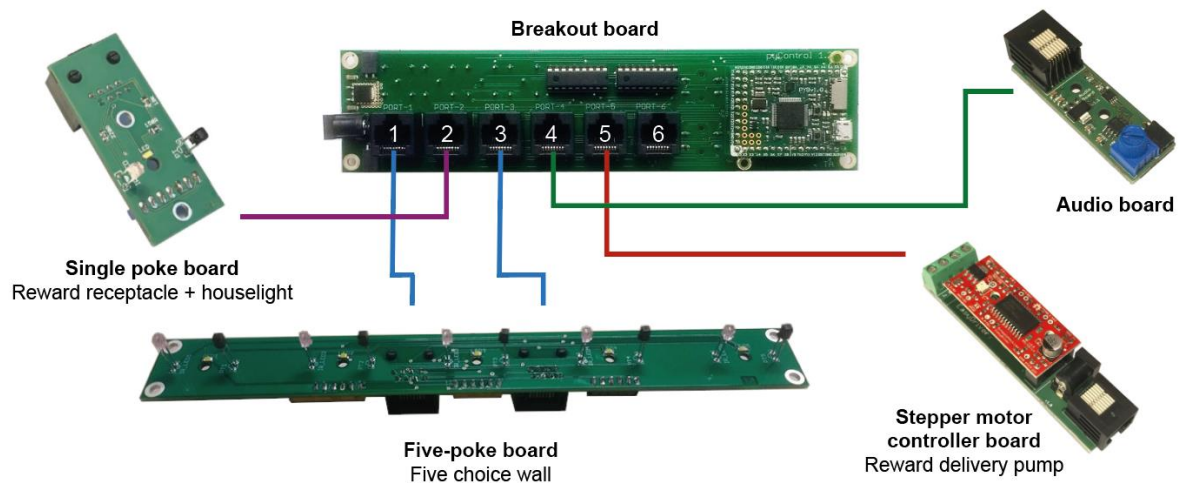
- 712 Akam, T., Rodrigues-Vaz, I., Marcelo, I., Zhang, X., Pereira, M., Oliveira, R.F., Dayan, P.,  
713 and Costa, R.M. (2020). The Anterior Cingulate Cortex Predicts Future States to Mediate  
714 Model-Based Action Selection. *Neuron* 0.
- 715 Ayaz, A., Stäuble, A., Hamada, M., Wulf, M.-A., Saleem, A.B., and Helmchen, F. (2019).  
716 Layer-specific integration of locomotion and sensory information in mouse barrel cortex. *Nat.*  
717 *Commun.* 10, 2585.
- 718 Baker, M. (2016). 1,500 scientists lift the lid on reproducibility. *Nat. News* 533, 452.
- 719 Bari, A., Dalley, J.W., and Robbins, T.W. (2008). The application of the 5-choice serial  
720 reaction time task for the assessment of visual attentional processes and impulse control in  
721 rats. *Nat. Protoc.* 3, 759–767.
- 722 Bhagat, J., Wells, M.J., Harris, K.D., Carandini, M., and Burgess, C.P. (2020). Rigbox: An  
723 Open-Source Toolbox for Probing Neurons and Behavior. *ENeuro* 7.
- 724 Buscher, N., Ojeda, A., Francoeur, M., Hulyalkar, S., Claros, C., Tang, T., Terry, A., Gupta,  
725 A., Fakhraei, L., and Ramanathan, D.S. (2020). Open-source raspberry Pi-based operant  
726 box for translational behavioral testing in rodents. *J. Neurosci. Methods* 342, 108761.
- 727 Carli, M., Robbins, T.W., Evenden, J.L., and Everitt, B.J. (1983). Effects of lesions to  
728 ascending noradrenergic neurones on performance of a 5-choice serial reaction task in rats;  
729 implications for theories of dorsal noradrenergic bundle function based on selective attention  
730 and arousal. *Behav. Brain Res.* 9, 361–380.
- 731 Chagas, A.M. (2018). Haves and have nots must find a better way: The case for open  
732 scientific hardware. *PLOS Biol.* 16, e3000014.
- 733 Chong, E.Z., Panniello, M., Barreiros, I., Kohl, M.M., and Booth, M.J. (2019). Quasi-  
734 simultaneous multiplane calcium imaging of neuronal circuits. *Biomed. Opt. Express* 10,  
735 267–282.
- 736 Devarakonda, K., Nguyen, K.P., and Kravitz, A.V. (2016). ROBucket: A low cost operant  
737 chamber based on the Arduino microcontroller. *Behav. Res. Methods* 48, 503–509.
- 738 Fitzpatrick, C.M., and Andreasen, J.T. (2019). Differential effects of ADHD medications on  
739 impulsive action in the mouse 5-choice serial reaction time task. *Eur. J. Pharmacol.* 847,  
740 123–129.
- 741 Grimm, C.M., Aksamaz, S., Schulz, S., Teutsch, J., Sicinski, P., Liss, B., and Kätzel, D.  
742 (2018). Schizophrenia-related cognitive dysfunction in the Cyclin-D2 knockout mouse model  
743 of ventral hippocampal hyperactivity. *Transl. Psychiatry* 8, 1–16.
- 744 Gurley, K. (2019). Two open source designs for a low-cost operant chamber using  
745 Raspberry Pi™. *J. Exp. Anal. Behav.* 111, 508–518.
- 746 International Brain Laboratory, Aguillon-Rodriguez, V., Angelaki, D.E., Bayer, H.M.,  
747 Bonacchi, N., Carandini, M., Cazes, F., Chapuis, G.A., Churchland, A.K., Dan, Y., et al.  
748 (2020). A standardized and reproducible method to measure decision-making in mice.  
749 *BioRxiv* 2020.01.17.909838.

- 750 Kim, B., Kenchappa, S.C., Sunkara, A., Chang, T.-Y., Thompson, L., Doudlah, R., and  
751 Rosenberg, A. (2019). Real-time experimental control using network-based parallel  
752 processing. *ELife* 8, e40231.
- 753 Koralek, A.C., and Costa, R.M. (2020). Sustained dopaminergic plateaus and noradrenergic  
754 depressions mediate dissociable aspects of exploitative states. *BioRxiv* 822650.
- 755 Korn, C., Akam, T., Jensen, K.H., Vagnoni, C., Huber, A., Tunbridge, E.M., and Walton, M.E.  
756 (2019). Distinct roles for DAT and COMT in regulating dopamine transients and reward-  
757 guided decision making. *BioRxiv* 823401.
- 758 Krakauer, J.W., Ghazanfar, A.A., Gomez-Marin, A., MacIver, M.A., and Poeppel, D. (2017).  
759 Neuroscience Needs Behavior: Correcting a Reductionist Bias. *Neuron* 93, 480–490.
- 760 Lopes, G., Bonacchi, N., Frazão, J., Neto, J.P., Atallah, B.V., Soares, S., Moreira, L., Matias,  
761 S., Itskov, P.M., Correia, P.A., et al. (2015). Bonsai: an event-based framework for  
762 processing and controlling data streams. *Front. Neuroinformatics* 9.
- 763 Marder, E. (2013). The haves and the have nots. *ELife* 2, e01515.
- 764 Márquez, C., Rennie, S.M., Costa, D.F., and Moita, M.A. (2015). Prosocial Choice in Rats  
765 Depends on Food-Seeking Behavior Displayed by Recipients. *Curr. Biol.* 25, 1736–1745.
- 766 Navarra, R., Graf, R., Huang, Y., Logue, S., Comery, T., Hughes, Z., and Day, M. (2008).  
767 Effects of atomoxetine and methylphenidate on attention and impulsivity in the 5-choice  
768 serial reaction time test. *Prog. Neuropsychopharmacol. Biol. Psychiatry* 32, 34–41.
- 769 Nelson, A., Abdelmesih, B., and Costa, R.M. (2020). Corticospinal neurons encode complex  
770 motor signals that are broadcast to dichotomous striatal circuits. *BioRxiv*  
771 2020.08.31.275180.
- 772 O'Connor, D.H., Clack, N.G., Huber, D., Komiyama, T., Myers, E.W., and Svoboda, K.  
773 (2010). Vibrissa-Based Object Localization in Head-Fixed Mice. *J. Neurosci.* 30, 1947–1967.
- 774 O'Leary, J.D., O'Leary, O.F., Cryan, J.F., and Nolan, Y.M. (2018). A low-cost touchscreen  
775 operant chamber using a Raspberry Pi™. *Behav. Res. Methods* 50, 2523–2530.
- 776 Paterson, N.E., Ricciardi, J., Wetzler, C., and Hanania, T. (2011). Sub-optimal performance  
777 in the 5-choice serial reaction time task in rats was sensitive to methylphenidate,  
778 atomoxetine and d-amphetamine, but unaffected by the COMT inhibitor tolcapone. *Neurosci.*  
779 *Res.* 69, 41–50.
- 780 Pillidge, K., Porter, A.J., Vasili, T., Heal, D.J., and Stanford, S.C. (2014). Atomoxetine  
781 reduces hyperactive/impulsive behaviours in neurokinin-1 receptor 'knockout' mice.  
782 *Pharmacol. Biochem. Behav.* 127, 56–61.

783

784

785 **Supplementary Figures**



786

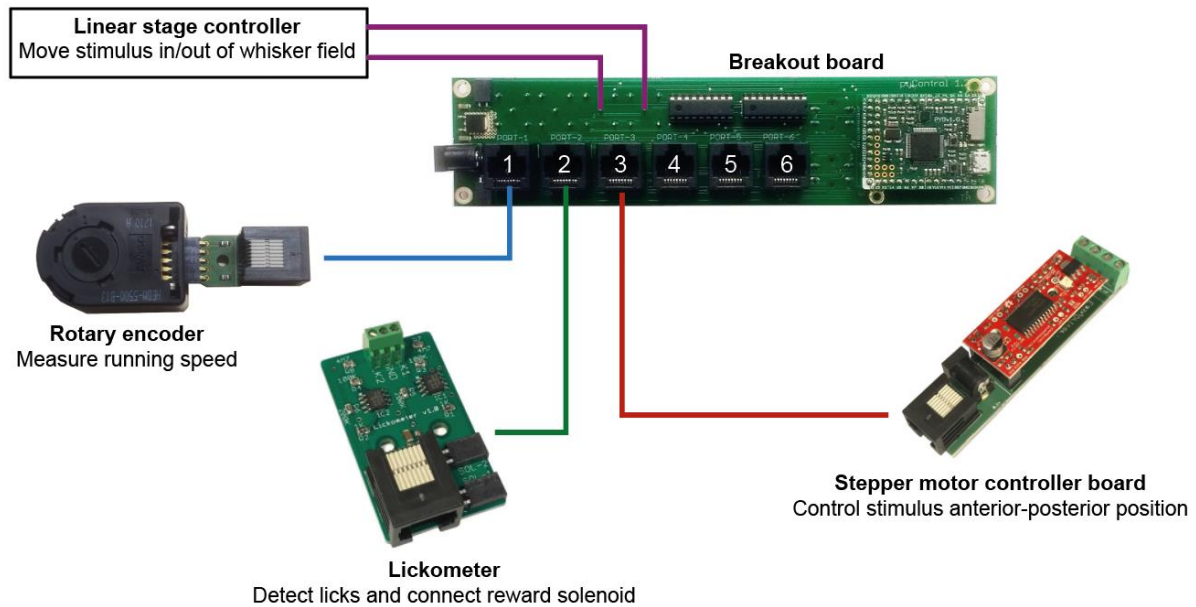
787 **Figure S1 (related to figure 6). Hardware configuration for 5-choice serial reaction time task.**

788 Diagram of hardware modules used to implement the 5-CSRT task. A breakout board is connected to  
789 a Five-poke board which integrates the IR beams and LEDs for the ports on the 5 choice wall onto a  
790 single PCB controlled from two behaviour ports, a stepper motor controller is used with a custom made  
791 3D printed peristaltic pump for reward delivery, a single poke board is used for the reward receptacle  
792 with a 12v LED module used for house light connected to its solenoid output connector, and an audio  
793 board for generating auditory stimuli. The hardware definition for this setup is:

```
from devices import *  
  
board = Breakout_1_2() # Instantiate breakout board.  
  
# Instantiate Five Poke board connected to breakout board ports 1 and 3.  
five_poke = Five_poke(ports=[board.port_1, board.port_3])  
  
# Instantiate reward port poke board connected to breakout board port 2.  
reward_port = Poke(port=board.port_2, rising_event='poke_6',  
                   falling_event='poke_6_out')  
  
# Instantiate audio board connected to breakout board port 4.  
speaker = Audio_board(port=board.port_4)  
  
# Instantiate syringe pump stepper motor connected to breakout board port 5.  
syringe_pump = Stepper_motor(port=board.port_5)  
  
# House light is connected to reward port's solenoid output.  
house_light = reward_port.SOL
```

794

795



796

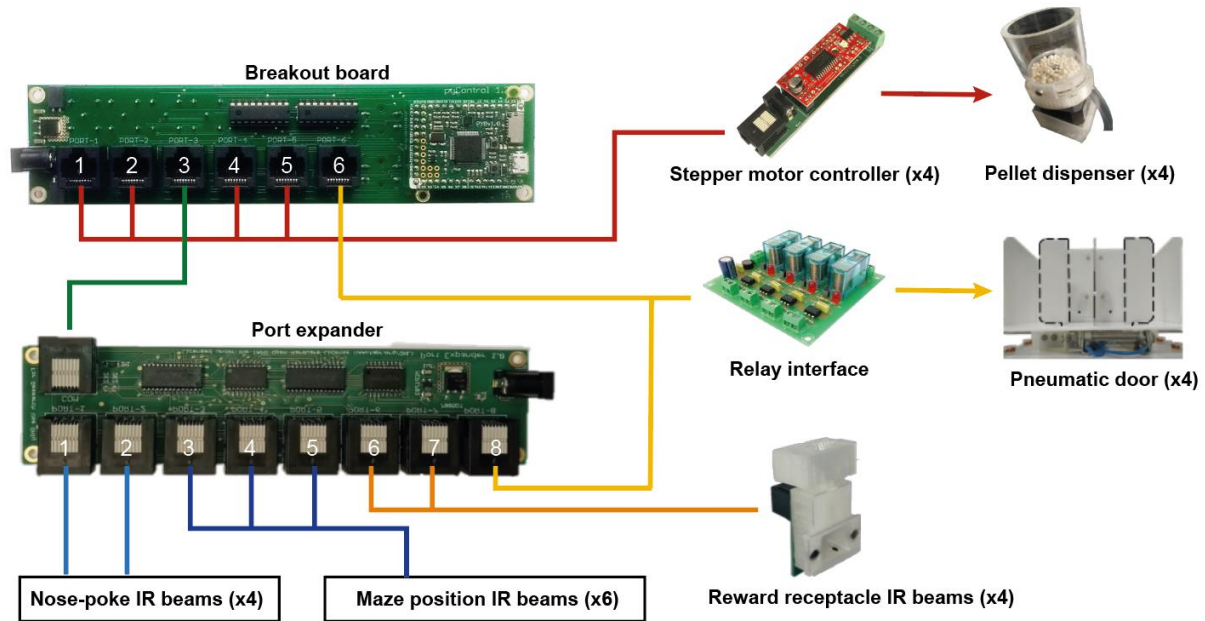
797 **Figure S2 (related to figure 7). Hardware configuration for vibrissae-based object localisation**  
798 **task.** Diagram of the hardware modules used to implement the head-fixed vibrissae-based object  
799 localisation task. A breakout board is connected to a rotary encoder module, used to measure running  
800 speed, a lickometer, used to detect licks and control the reward solenoid, a stepper motor controller  
801 used to set the anterior-posterior position of the stimulus, and a controller for the linear stage used to  
802 move the stimulus in and out of the whisker field. The hardware definition for this setup is:

```
from devices import *  
  
board = Breakout_1_2() # Instantiate breakout board.  
  
# Instantiate Rotary encoder (currently only supported on port 1).  
running_wheel = Rotary_encoder(name='running_wheel', sampling_rate=30,  
                               output='velocity')  
  
# Instantiate lickometer connected to breakout board port 2.  
Lickometer = Lickometer(port=board.port_2, rising_event_A='lick_event')  
  
# Instantiate stepper motor controller connected to breakout board port 3.  
stepper = Stepper_motor(port=board.port_3)  
  
# Instantiate digital outputs used to control linear stage on BNC connectors.  
linearStage_forwardTrig = Digital_output(pin=board.BNC_1)  
linearStage_backwardTrig = Digital_output(pin=board.BNC_2)
```

803

804

805



806

807 **Figure S3 (related to figure 8). Hardware configuration for social decision making task.** Diagram  
 808 of the hardware modules used to implement the double T maze apparatus for the social decision making  
 809 task. A port expander is used to provide additional IO lines for IR beams, stepper motor controller  
 810 boards are used to control custom made pellet dispensers, and a relay interface board is used to control  
 811 the solenoids actuating the pneumatic doors. The hardware definition for this setup is:

```

from devices import *

# Instantiate Breakout board
board = Breakout_1_2()

# Instantiate Port Expander.
port_exp = Port_expander(board.port_3)

# Instantiate stepper motors used for reward delivery.
motor_1A = Stepper_motor(board.port_1)
motor_1B = Stepper_motor(board.port_2)
motor_2A = Stepper_motor(board.port_4)
motor_2B = Stepper_motor(board.port_5)

# Instantiate pokes for decision and food-seeking behaviour. Uses a non-standard poke
# design in which two IR beam and LED pairs are connected to a single port.
poke_1A = PokeA(port_exp.port_1, rising_event='poke_1A', falling_event='poke_1A_out')
poke_1B = PokeB(port_exp.port_1, rising_event='poke_1B', falling_event='poke_1B_out')
poke_2A = PokeA(port_exp.port_2, rising_event='poke_2A', falling_event='poke_2A_out')
poke_2B = PokeB(port_exp.port_2, rising_event='poke_2B', falling_event='poke_2B_out')

# Instantiate IR detectors for subjects location in maze.
IR_1A = PokeA(port_exp.port_3, rising_event='IR_1A', falling_event='IR_1A_out')
IR_1B = PokeB(port_exp.port_3, rising_event='IR_1B', falling_event='IR_1B_out')
IR_1C = PokeA(port_exp.port_4, rising_event='IR_1C', falling_event='IR_1C_out')
IR_2A = PokeB(port_exp.port_4, rising_event='IR_2A', falling_event='IR_2A_out')
IR_2B = PokeA(port_exp.port_5, rising_event='IR_2B', falling_event='IR_2B_out')
IR_2C = PokeB(port_exp.port_5, rising_event='IR_2C', falling_event='IR_2C_out')

# Instantiate reward receptacles.
feeder_1A = PokeA(port_exp.port_6, rising_event='feeder_1A', falling_event='feeder_1A_out')
feeder_1B = PokeB(port_exp.port_6, rising_event='feeder_1B', falling_event='feeder_1B_out')
feeder_2A = PokeA(port_exp.port_7, rising_event='feeder_2A', falling_event='feeder_2A_out')
    
```



```
feeder_2B = PokeB(port_exp.port_7, rising_event='feeder_2B', falling_event='feeder_2B_out')
```

```
# Instantiate doors (digital outputs)
```

```
door_1A = Digital_output(pin=board.port_6.POW_A)
```

```
door_1B = Digital_output(pin=board.port_6.POW_B)
```

```
door_2A = Digital_output(pin=port_exp.port_8.POW_A)
```

```
door_2B = Digital_output(pin=port_exp.port_8.POW_B)
```

812

813